



Cite this: *Chem. Commun.*, 2025, 61, 7446

Received 3rd March 2025,  
Accepted 17th April 2025

DOI: 10.1039/d5cc01141h

rsc.li/chemcomm

# A triosmium carbonyl cluster that inhibits $\alpha$ -synuclein aggregation and disassembles preformed aggregates†

Xin Liang,<sup>a</sup> Balasz Gulyas,<sup>b</sup> Mathangi Palanivel<sup>id</sup><sup>b</sup> and Weng Kee Leong<sup>id</sup><sup>\*a</sup>

Two triosmium carbonyl clusters, viz.,  $\text{Os}_3(\mu\text{-H})(\mu\text{-SC}_6\text{H}_4\text{-p-NO}_2)(\text{CO})_{10}$  (**1**) and  $\text{Os}_3(\mu\text{-H})(k\text{O},\mu\text{-O}'\text{-2-flavone})(\text{CO})_9$  (**2**), effectively inhibited  $\alpha$ -synuclein aggregation, a key signature of Parkinson's disease (PD), in both wild-type and A53T-mutant  $\alpha$ -synuclein models. Cluster **2** showed superior efficacy and a significantly better safety profile, and could also disassemble preformed aggregates.

Parkinson's disease (PD) is a progressive neurodegenerative disorder that can affect motor functions, leading to life-threatening complications such as pneumonia in its advanced stages.<sup>1–3</sup> Diagnosis is typically based on motor dysfunction and tremors, which may not be prominent in the early stages, making it challenging for individuals with non-motor symptoms. There is currently no treatment available to reverse progression; hence, early intervention strategies for halting or reversing advanced PD are highly desirable.<sup>4–11</sup> One biochemical hallmark of PD is the abnormal aggregation of  $\alpha$ -synuclein to form toxic inclusions known as Lewy bodies.<sup>12–18</sup> Targeting the aggregation of  $\alpha$ -synuclein or promoting the disassembly of its aggregates are among the promising therapeutic approaches.<sup>14–16</sup> One strategy to modulate  $\alpha$ -synuclein aggregation is through small molecule inhibitors and some, such as **Anle138b** and **NPT200-11**, have reached clinical trials (Fig. 1).<sup>17–23</sup> Their ring systems appear to be essential as studies have indicated that even compounds with a single ring can effectively inhibit  $\alpha$ -synuclein aggregation;<sup>24</sup> for example, **ZPDm** has been shown to both inhibit  $\alpha$ -synuclein aggregation and disassemble preformed fibrils.<sup>25</sup>

Metal-based compounds have found potential in biomedicine, including the ruthenium complex **NAMI-A**, which has also

been shown to exhibit potential as a therapeutic agent for PD.<sup>26–46</sup> The larger ligand sphere in di- and multi-nuclear complexes may be expected to offer greater potential for incorporating multi-target or -drug capabilities; their larger molecular size may also help reduce protein–protein interactions and aggregation. In this paper, we report on our investigations into the potential of two triosmium carbonyl clusters, viz.,  $\text{Os}_3(\mu\text{-H})(\mu\text{-SC}_6\text{H}_4\text{-p-NO}_2)(\text{CO})_{10}$  (**1**) and  $\text{Os}_3(\mu\text{-H})(k\text{O},\mu\text{-O}'\text{-2-flavone})(\text{CO})_9$  (**2**), for PD treatment (Scheme 1).

In our previous SAR studies, we have found that the cytotoxicity of triosmium carbonyl clusters such as **1** is associated with the formation of a vacant site on the triosmium core for binding of a biomolecule; factors that affect this would impact cytotoxicity.<sup>47</sup> We conjectured that replacement of the bridging moiety (O for S) and of the aromatic ring with a larger ring system may further reduce cytotoxicity; the latter should also strengthen interaction with  $\alpha$ -synuclein. Both clusters have been fully characterized spectroscopically (IR, NMR, HRMS) and by single-crystal X-ray crystallography. The structure of **1** has already been reported;<sup>47</sup> an ORTEP plot for **2** is shown in Fig. 2. The pattern for the CO vibrations in the IR spectrum and the metal hydride resonance at  $-9.27$  ppm in the  $^1\text{H}$  NMR spectrum of cluster **2** are consistent with those reported for triosmium carbonyl clusters containing hydroxypyrrone.<sup>48</sup> Its UV absorption spectrum exhibits bands typical of flavonoids, with absorption maxima in the 240–270 nm and 320–380 nm ranges, along with an additional band at 520 nm (Fig. S3, ESI†),<sup>49–52</sup> while the emission spectrum shows a single emission peak at  $\sim 540$  nm under 350 nm excitation, which is attributable to a charge transfer (CT) band (Fig. S4, ESI†); the

<sup>a</sup> Division of Chemistry and Biological Chemistry, School of Chemistry, Chemical Engineering and Biotechnology, Nanyang Technological University, Singapore 637371, Singapore. E-mail: chmlwk@ntu.edu.sg

<sup>b</sup> Lee Kong Chian School of Medicine, Nanyang Technological University, 59 Nanyang Drive, Singapore 636921, Singapore

† Electronic supplementary information (ESI) available. CCDC 2426212. For ESI and crystallographic data in CIF or other electronic format see DOI: <https://doi.org/10.1039/d5cc01141h>

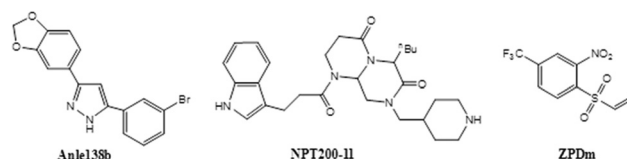
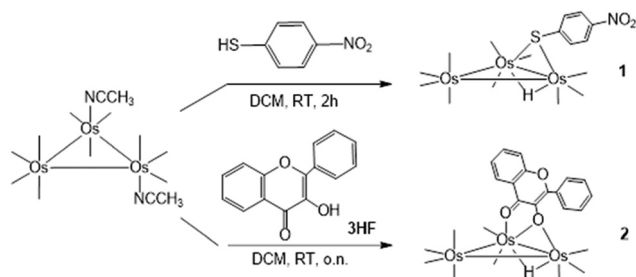
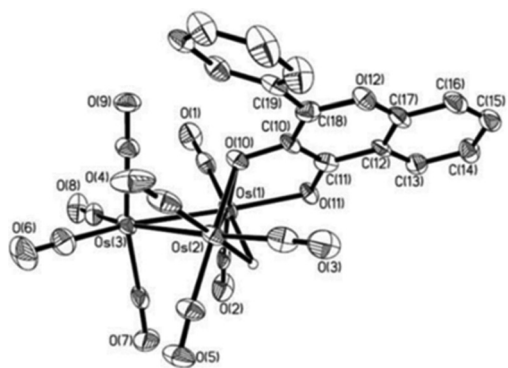


Fig. 1 Known small molecule inhibitors for the treatment of PD.





**Scheme 1** Synthesis of clusters **1** and **2**. Short lines denote terminal CO ligands.



**Fig. 2** ORTEP plot showing the molecular structure of cluster **2**, with thermal ellipsoids drawn at the 50% probability level. All organic H atoms have been omitted. Selected bond distances (Å) and bond angles (deg): Os(1)–Os(2) = 2.8152(5), Os(1)–Os(3) = 2.7679(5), Os(2)–Os(3) = 2.8282(5), Os(1)–O(11) = 2.158(5), Os(1)–O(10) = 2.146(5), Os(2)–O(10) = 2.175(5), Os(2)–O(10)–Os(1) = 81.32(19).

color of the solution is solvent-dependent, changing from yellow-orange in DCM to dark red in DMSO.

MTT assays carried out on clusters **1** and **2** against the SH-SY5Y cell line (human-derived neuroblastoma) commonly used in Parkinson's disease (PD) studies showed that **2** was significantly less cytotoxic than **1**; no signs of cytotoxicity were observed up to at least 50  $\mu\text{M}$  for the former, while an  $\text{IC}_{50}$  of  $28 \pm 6 \mu\text{M}$  was determined for the latter (Fig. S5, ESI<sup>†</sup>). The latter  $\text{IC}_{50}$  value is also worth comparing with a value of  $72 \pm 8 \mu\text{M}$  against triple negative breast carcinoma (MDA-MB-231) under the same treatment conditions.<sup>42</sup>

The inhibitory efficacy of **1** and **2** on wild-type  $\alpha$ -synuclein aggregation (the form most commonly associated with PD) was assessed through a thioflavin T (ThT) fluorescence assay, with curcumin, a well-established compound for preventing aggregation in  $\alpha$ -synuclein, as a positive control.<sup>53–57</sup> The results showed that the inhibitory effect of both clusters was immediate and sustained, and superior to that of curcumin (Fig. 3 and Fig. S8, ESI<sup>†</sup>). Inhibition of aggregation was also visible in the transmission electron microscopy (TEM) images, which showed that the treated samples exhibited remarkably fewer aggregates, with smaller and shorter structures, compared to the untreated sample (negative control) which showed amyloid fibrils as long,

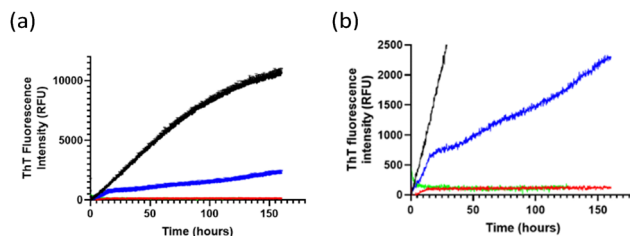


**Fig. 3** (a) Plot of ThT (20  $\mu\text{M}$ ) fluorescence intensity against time for clusters **1** (red) and **2** (green), and curcumin (blue, positive control) for the aggregation of  $\alpha$ -synuclein (100  $\mu\text{g mL}^{-1}$ ); untreated  $\alpha$ -synuclein (100  $\mu\text{g mL}^{-1}$ , negative control) in black. (b) Magnified view of fluorescence intensity from 0 to 2500 RFU.

twisted filamentous structures approximately 7–10 nm in diameter (Fig. S6, ESI<sup>†</sup>). The inhibitory effects were also concentration-dependent, with **2** exhibiting slightly higher efficacy; an optimal inhibitory concentration of 10–20  $\mu\text{M}$  reaching  $\sim 92\%$  inhibition at 20  $\mu\text{M}$ , was obtained, as compared to 20–40  $\mu\text{M}$  for **1** (Fig. S7, ESI<sup>†</sup>). This optimal inhibitory concentration of **2** was well below its cytotoxicity range. The fact that the inhibitory efficacy of **2** was significantly greater than that for free 3HF also suggested that the cluster core played a role in the inhibition of aggregation.

The inhibitory effect of **2** on A53T mutant  $\alpha$ -synuclein aggregation was also examined; this mutation is linked to genetically inherited PD and is characterized by the formation of toxic fibrils at a much faster rate than wild-type  $\alpha$ -synuclein.<sup>58–60</sup> The results were surprisingly promising; while the optimal inhibitory concentration remained the same as for the wild type (10–20  $\mu\text{M}$ ), it demonstrated greater efficacy at lower concentrations (Fig. 4). Notably, at 5  $\mu\text{M}$  concentration, there was a significant drop in inhibition compared to the wild type ( $\sim 50\%$  and  $26\%$ , respectively). Thus, **2** is effective in inhibiting aggregation of both wild-type and A53T mutant  $\alpha$ -synuclein.

The *in vivo* inhibition of  $\alpha$ -synuclein aggregation was also evaluated using an immunofluorescence assay (IFA) on SH-SY5Y cells overexpressing A53T-mutated  $\alpha$ -synuclein, with aggregation induced by rotenone, a widely used environmental toxicant in Parkinson's disease research to mimic neurodegenerative conditions.<sup>61–64</sup> The results show that cells treated with **1** or **2** exhibited negligible aggregate formation compared to the negative control (Fig. 5).

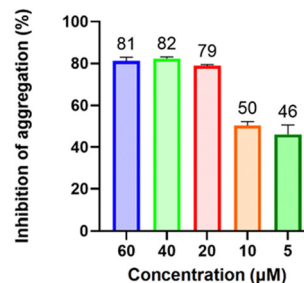


**Fig. 4** Inhibition of A53T mutant  $\alpha$ -synuclein aggregation after treatment with varying concentrations of **2**.



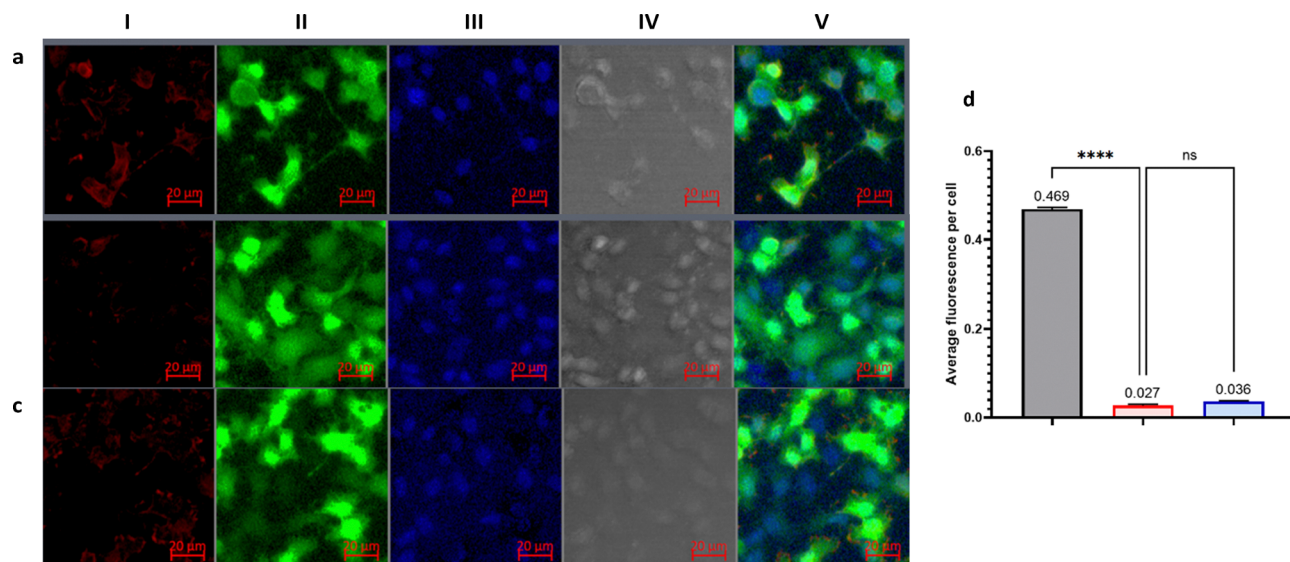


**Fig. 5** IFA analysis of  $\alpha$ -synuclein aggregation in A53T mutant SH-SY5Y cells. Column (I)  $\alpha$ -synuclein aggregates stained with anti- $\alpha$ -synuclein aggregate antibody, (II) EGFP-tagged A53T-mutated  $\alpha$ -synuclein, (III) DAPI-stained nuclei, (IV) bright-field image, and (V) merged image of all channels. Row: (a) untreated cells (negative control), (b) treated with **2** (white circle highlights faint red signal), (c) treated with **1**, and (d) quantification of red and green fluorescence colocalization, normalized to nuclear count.

The disassembly of preformed fibrils is a desirable outcome for reversing the effects of Parkinson's disease (PD) and is particularly crucial in late-stage PD. We have found that **2** could effectively disassemble preformed fibrils, including those formed by A53T mutant  $\alpha$ -synuclein. This may be attributable to the presence of the aromatic ring system, which facilitates  $\pi$ - $\pi$  interactions with aromatic residues in  $\alpha$ -synuclein fibrils, such as tyrosine, phenylalanine, and tryptophan.<sup>65</sup> Additionally, the bulky nature of the triosmium core introduces steric strain and hydrophobic interactions, leading to local structural perturbations and increasing the susceptibility of aggregates to disassemble.<sup>66</sup> This is supported by the observation that while 20  $\mu$ M of **3HF** resulted in only 10% disassembly, it was 33% disassembly with **2** even at 5  $\mu$ M concentration (Fig. 6). Our findings thus suggest that the triosmium cluster core plays a critical role in disrupting the stabilizing forces within the fibrils, effectively promoting their breakdown.

In this study, we have shown that the triosmium carbonyl clusters **1** and **2** could inhibit the aggregation of  $\alpha$ -synuclein,

with **2** also capable of disassembling preformed aggregates. This effect was observed in both wild-type and A53T mutant  $\alpha$ -synucleins. Notably, **2** exhibited optimal activity at concentrations well below that at which any antiproliferative effects could be observed. We propose that the metal cluster core plays an important role in its activity and while the precise mode of action remains unclear, these findings suggest that compounds of this type hold great potential for further development.

Funding support from the Ministry of Education, Singapore, through the university research grants RG12/20 and RG1/21 is gratefully acknowledged.

## Data availability

The data supporting this article have been included as part of the ESI.† Crystallographic data for **2** has been deposited with the Cambridge Crystallographic Data Centre as CCDC 2426212.†

## Conflicts of interest

We declare that there are no conflicts of interest.

## References

- 1 J. Jankovic and E. K. Tan, *J. Neurol., Neurosurg. Psychiatry*, 2020, **91**, 795.
- 2 D. Aarsland, L. Batzu, G. M. Halliday, G. J. Geurtsen, C. Ballard, K. Ray Chaudhuri and D. Weintraub, *Nat. Rev. Dis. Primers*, 2021, **7**, 47.
- 3 G. DeMaagd and A. Philip, *Pharm. Ther.*, 2015, **40**, 504.
- 4 C. Kobylecki, *Clin. Med.*, 2020, **20**, 393.
- 5 J. Fujikawa, R. Morigaki, N. Yamamoto, H. Nakanishi, T. Oda, Y. Izumi and Y. Takagi, *Life*, 2023, **13**, 78.
- 6 X. Dong-Chen, C. Yong, X. Yang, S. Chen-Yu and P. Li-Hua, *Signal Transduction Targeted Ther.*, 2023, **8**, 73.
- 7 R. N. Rees, A. P. Acharya, A. Schrag and A. J. Noyce, *F1000Res*, 2018, **7**, 1106.

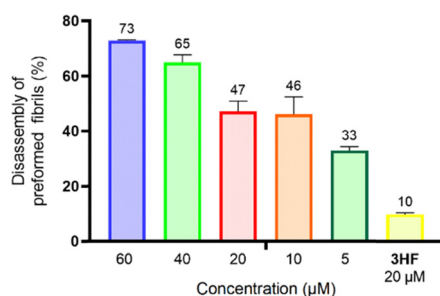


**Fig. 6** Disassembly of preformed A53T mutant  $\alpha$ -synuclein fibrils following treatment with varying concentrations of **2**, with **3HF** (20  $\mu$ M) as a positive control.



- 8 V. Carroll, R. Rossiter and D. Blanchard, *Aust. J. Gen. Pract.*, 2021, **50**, 812.
- 9 R. Armañanzas, C. Bielza, K. R. Chaudhuri, P. Martinez-Martin and P. Larrañaga, *Artif. Intell. Med.*, 2013, **58**, 195.
- 10 T. Pardo-Moreno, V. García-Morales, S. Suleiman-Martos, A. Rivas-Dominguez, H. Mohamed-Mohamed, J. J. Ramos-Rodriguez, L. Melguizo-Rodríguez and A. González-Acedo, *Pharmaceutics*, 2023, **15**, 770.
- 11 Y. Wu, X. Meng, W.-Y. Cheng, Z. Yan, K. Li, J. Wang, T. Jiang, F. Zhou, K.-H. Wong and C. Zhong, *et al.*, *Front. Neurosci.*, 2024, **18**, 1210447.
- 12 M. Sharma and J. Burré, *Trends Neurosci.*, 2023, **46**, 153.
- 13 J. Burré, *J. Parkinsons Dis.*, 2015, **5**, 699.
- 14 D. Baggett, A. Olson and M. S. Parmar, *Brain Disord.*, 2024, **16**, 100163.
- 15 C. R. Fields, N. Bengoa-Vergniory and R. Wade-Martins, *Front. Mol. Neurosci.*, 2019, **12**, 299.
- 16 M. Vidović and M. G. Rikalovic, *Cells*, 2022, **11**, 1732.
- 17 G. Henriquez and M. Narayan, *Explor. Neuroprotect. Ther.*, 2023, **3**, 207.
- 18 I. M. Sandoval, D. J. Marmion, K. T. Meyers and F. P. Manfredsson, *J. Parkinsons Dis.*, 2021, **11**, S189–S197.
- 19 M. Izco, J. Blesa, M. Schlee, M. Schmeer, R. Porcari, R. Al-Shawi, S. Ellmerich, M. de Toro, C. Gardiner and Y. Seow, *et al.*, *Mol. Ther.*, 2019, **27**, 2111.
- 20 J. S. Lee and S. J. Lee, *J. Mov. Disord.*, 2016, **9**, 14.
- 21 B. Xiao and E.-K. Tan, *J. Transl. Med.*, 2023, **21**, 178.
- 22 J. Levin, N. Sing, S. Melbourne, A. Morgan, C. Mariner, M. G. Spillantini, M. Wegrzynowicz, J. W. Dalley, S. Langer and S. Ryazanov, *et al.*, *eBioMedicine*, 2022, **80**, 104021.
- 23 D. L. Price, A. Khan, R. Angers, A. Cardenas, M. K. Prato, M. Bani, D. W. Bonhaus, M. Citron and A.-L. Biere, *npj Parkinson's Dis.*, 2024, **10**, 60.
- 24 D. S. Pena and S. Ventura, *Neural Regen. Res.*, 2022, **17**, 508.
- 25 S. Peña-Díaz, J. Pujols, F. Pinheiro, J. Santos, I. Pallarés, S. Navarro, M. Conde-Gimenez, J. García, X. Salvatella and E. Dalfó, *et al.*, *Front. Bioeng. Biotechnol.*, 2020, **8**, 588947.
- 26 T. A. Sales, I. G. Prandi, A. A. de Castro, D. H. S. Leal, E. F. F. da Cunha, K. Kuca and T. C. Ramalho, *Int. J. Mol. Sci.*, 2019, **20**, 1829.
- 27 E. Carboni and P. Lingor, *Metallomics*, 2015, **7**, 395.
- 28 R. Moons, A. Konijnenberg, C. Mensch, R. Van Elzen, C. Johannessen, S. Maudsley, A.-M. Lambeir and F. Sobott, *Sci. Rep.*, 2020, **10**, 16293.
- 29 F. Schifano, S. Dell'Acqua, S. Nicolis, L. Casella and E. Monzani, *Antioxidants*, 2023, **12**, 791.
- 30 A. Binolfi, L. Quintanar, C. W. Bertocini, C. Griesinger and C. O. Fernández, *Coord. Chem. Rev.*, 2012, **256**, 2188.
- 31 V. N. Uversky, J. Li and A. L. Fink, *J. Biol. Chem.*, 2001, **276**, 44284.
- 32 Z. Jansen van Rensburg, S. Abrahams, S. Bardien and C. Kenyon, *Mol. Neurobiol.*, 2021, **58**, 5920.
- 33 A. Wypijewska, J. Galazka-Friedman, E. R. Bauminger, Z. K. Wszolek, K. J. Schweitzer, D. W. Dickson, A. Jaklewicz, D. Elbaum and A. Friedman, *Parkinsonism Relat. Disord.*, 2010, **16**, 329.
- 34 B. Chen, X. Wen, H. Jiang, J. Wang, N. Song and J. Xie, *Free Radic. Biol. Med.*, 2019, **141**, 253.
- 35 Q. Zhao, Y. Tao, K. Zhao, Y. Ma, Q. Xu, C. Liu, S. Zhang and D. Li, *J. Mol. Biol.*, 2023, **435**, 167680.
- 36 R. J. Ward, D. T. Dexter, A. Martin-Bastida and R. R. Crichton, *Int. J. Mol. Sci.*, 2021, **22**, 3338.
- 37 R. B. Mounsey and P. Teismann, *Int. J. Cell Biol.*, 2012, **2012**, 983245.
- 38 K. Cao, Y. Zhu, Z. Hou, M. Liu, Y. Yang, H. Hu, Y. Dai, Y. Wang, S. Yuan, G. Huang, J. Mei, P. J. Sadler and Y. Liu, *Angew. Chem.*, 2023, **135**, e202215360.
- 39 I. Tolbatov, E. Barresi, S. Taliani, D. La Mendola, T. Marzo and A. Marrone, *Inorg. Chem. Front.*, 2023, **10**, 2226.
- 40 S. La Manna, C. Di Natale, V. Panzetta, M. Leone, F. A. Mercurio, I. Cipollone, M. Monti, P. A. Netti, G. Ferraro and A. Terán, *et al.*, *Inorg. Chem.*, 2024, **63**, 564.
- 41 E. Meggers, *Chem. Commun.*, 2009, 1001.
- 42 A. Temesgen, H. C. Ananda Murthy, A. Z. Enyew, R. Revathi and R. Venkatesha Perumal, *Chem. Select*, 2023, **8**, e202302113.
- 43 Z. Pei, L. Li, N. Yang, S. Sun, N. Jiang and L. Cheng, *Coord. Chem. Rev.*, 2024, **517**, 215969.
- 44 H. Jiang, L. Li, Z. Li and X. Chu, *Biomed. Microdevices*, 2024, **26**, 12.
- 45 S. Abdolmaleki, A. Aliabadi and S. Khaksar, *Coord. Chem. Rev.*, 2024, **501**, 215579.
- 46 S. Bhattacharya, T. Adon, K. Dsouza and H. Y. Kumar, *Chem. Select*, 2025, **10**, e202404147.
- 47 X. Liang and W. K. Leong, *J. Med. Chem.*, 2024, **67**(23), 20980.
- 48 H. Z. Lee, W. K. Leong, S. Top and A. Vessières, *ChemMedChem*, 2014, **9**, 1453.
- 49 X. Zhao, X. Li, S. Liang, X. Dong and Z. Zhang, *RSC Adv.*, 2021, **11**, 28851.
- 50 H. Gao and X. Wu, *Chem. Heterocycl. Compd.*, 2018, **54**, 125.
- 51 K. W. Fan, H. L. Luk and D. L. Phillips, *Molecules*, 2023, **28**, 3966.
- 52 V. I. Tomin and D. V. Ushakov, *Polym. Test.*, 2017, **64**, 77.
- 53 N. Ahsan, S. Mishra, M. K. Jain, A. Suroia and S. Gupta, *Sci. Rep.*, 2015, **5**, 9862.
- 54 B. Xu, J. Chen and Y. Liu, *ACS Omega*, 2022, **7**, 30281.
- 55 P. K. Singh, V. Kotia, D. Ghosh, G. M. Mohite, A. Kumar and S. K. Maji, *ACS Chem. Neurosci.*, 2013, **4**, 393.
- 56 B. Ahmad and L. J. Lapidus, *J. Biol. Chem.*, 2012, **287**, 9193.
- 57 Tinku, S. A. Shaikh, I. K. Priyadarsini and S. Choudhary, *J. Mol. Liq.*, 2024, **405**, 125063.
- 58 L. Narhi, S. J. Wood, S. Steavenson, Y. Jiang, G. M. Wu, D. Anafi, S. A. Kaufman, F. Martin, K. Sitney and P. Denis, *et al.*, *J. Biol. Chem.*, 1999, **274**, 9843.
- 59 M. Perni, A. van der Goot, R. Limbocker, T. J. van Ham, F. A. Aprile, C. K. Xu, P. Flagmeier, K. Thijssen, P. Sormanni and G. Fusco, *et al.*, *Front. Cell. Dev. Biol.*, 2021, **9**, 552549.
- 60 Y. Guan, X. Zhao, F. Liu, S. Yan, Y. Wang, C. Du, X. Cui, R. Li and C. X. Zhang, *Front. Cell. Neurosci.*, 2020, **14**, DOI: [10.3389/fncel.2020.00159](https://doi.org/10.3389/fncel.2020.00159).
- 61 T. Ranasinghe, Y. Seo, H.-C. Park, S.-K. Choe and S.-H. Cha, *J. Hazard. Mater.*, 2024, **480**, 136215.
- 62 L. Zou, Z. Che, K. Ding, C. Zhang, X. Liu, L. Wang, A. Li and J. Zhou, *Antioxidants*, 2023, **12**(5), 1134.
- 63 N. Xiong, J. Xiong, M. Jia, L. Liu, X. Zhang, Z. Chen, J. Huang, Z. Zhang, L. Hou and Z. Luo, *et al.*, *Behav. Brain Funct.*, 2013, **9**(1), 13.
- 64 I. O. Ishola, I. O. Awogbindin, T. G. Olubodun-Obadun, A. E. Olajiga and O. O. Adeyemi, *NeuroToxicol.*, 2023, **96**, 37.
- 65 Y. Zhou, Y. Yao, Z. Yang, Y. Tang and G. Wei, *Phys. Chem. Chem. Phys.*, 2023, **25**, 14471–14483.
- 66 G. A. De Oliveira, M. d A. Marques, C. Cruzeiro-Silva, Y. Cordeiro, C. Schuabb, A. H. Moraes, R. Winter, H. Oschkinat, D. Foguel and M. S. Freitas, *Sci. Rep.*, 2016, **6**, 37990.

